Materials and Design 164 (2019) 107546

Contents lists available at ScienceDirect

Materials and Design

journal homepage: www.elsevier.com/locate/matdes

Shock loading simulation using density-graded metallic foam projectiles

Lang Li [a,b], Bin Han [c,d,g,*], Si-Yuan He [f], Zhen-Yu Zhao [a,b], Rui Zhang [a,b], Qian-Cheng Zhang [a,e], Tian Jian Lu [b,e,**]

[a] State Key Laboratory for Strength and Vibration of Mechanical Structures, Xi'an Jiaotong University, Xi'an 710049, PR China
[b] State Key Laboratory of Mechanics and Control of Mechanical Structures, Nanjing University of Aeronautics and Astronautics, Nanjing 210016, PR China
[c] School of Mechanical Engineering, Xi'an Jiaotong University, Xi'an 710049, PR China
[d] School of Engineering, Brown University, Providence, RI 02912, USA
[e] MOE Key Laboratory for Multifunctional Materials and Structures, Xi'an Jiaotong University, Xi'an 710049, PR China
[f] State Key Laboratory of Bioelectronics, School of Biological Science & Medical Engineering, Southeast University, Nanjing 210096, PR China
[g] Research institute of Xi'an Jiaotong University, Zhejiang, Hangzhou 311215, China

HIGHLIGHTS

- Density-graded metallic foam projectiles can be used to simulate shock loadings with varying pulse shapes.
- The local crushing stress and local density within the shock front are key factors altering the pulse shapes.
- By considering pulse shapes, the shock loading simulation technique can be expanded to broader applications.

GRAPHICAL ABSTRACT

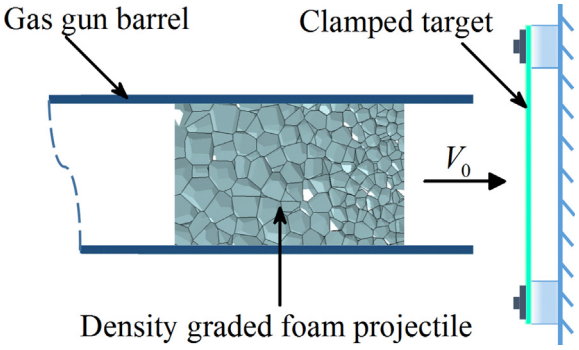

ARTICLE INFO

Article history:
Received 30 September 2018
Received in revised form 7 December 2018
Accepted 9 December 2018
Available online 14 December 2018

Keywords:
Density-graded foam projectile
Shock loading simulation
Pulse shape design

ABSTRACT

Density-graded metallic foam projectiles are proposed for shock loading simulation, with special focus placed upon designing pressure pulses having specific shapes. Experiments are performed to explore the potential of density-graded foam projectiles in generating shock loadings of various pulse shapes. Subsequently, three-dimensional Voronoi foam models with varying gradient profiles along the length direction are constructed for finite element (FE) simulations, which are validated against the experimental data. Then, FE simulations of density-graded foam projectiles impacting a stationary rigid wall are conducted to quantify the effect of density gradient on the shape of the pressure pulse generated and explore the physical mechanisms underlying such effect. It is demonstrated that density gradient affects significantly local crushing stress and local density within the shock front when it propagates from the impact end to the other end of the foam projectile. Inspired by the FE simulation results and the classical Taylor impact model, one-dimensional theoretical model for density-graded foam projectiles is developed to predict the contact force between the projectile and the fixed rigid wall. Finally, the theoretical model is employed to determine the geometry, density gradient, and firing velocity of foam projectiles needed to generate shock loadings with prescribed pulse shapes.

* Correspondence to: B. Han, School of Mechanical Engineering, Xi'an Jiaotong University, Xi'an 710049, PR China.
** Correspondence to: T.J. Lu, State Key Laboratory of Mechanics and Control of Mechanical Structures, Nanjing University of Aeronautics and Astronautics, Nanjing 210016, PR China.
E-mail addresses: hanbinghost@xjtu.edu.cn (B. Han), tjlu@nuaa.edu.cn (T.J. Lu).

https://doi.org/10.1016/j.matdes.2018.107546

1. Introduction

Shock-type loadings occur in air blast, water blast, collision of vehicles and impact [1], typically expressed by a pressure time history $p(t)$ with peak pressure P_{peak} and decay duration τ. As discussed by Jones [2], such loading may be considered to be dynamic if $\tau/T \ll 1$, where T is the response time of the structure; in the limit $\tau/T \to 0$, the loading is taken as impulsive. In the impulsive regime, the pressure-time history is commonly treated as an impulse of magnitude $I = \int_0^{\tau} p(t)dt$. Since there is not a strict boundary to distinguish the dynamic and impulse regimes, Jones [2] and Xue and Hutchinson [3] suggested that, for monolithic and sandwich panels, $\tau/T = 0.01$ may be approximately used to distinguish the two regimes. This viewpoint has since been widely approved, because treating the pressure time history as an impulse when $\tau/T \le 0.01$ causes little loss of accuracy so long as the overall response of the structure is of concern.

Therefore, in imparting a shock loading on the structure, two approaches are generally adopted: prescribed momentum and prescribed pressure time history. In the impulsive regime, the damage of the structure only depends on the impulse I and hence both approaches can define the shock loading. In contrast, beyond the impulsive regime, the structural damage depends not only on the impulse, but also on the pulse shape such as the peak pressure and the shape ratio which defines as the ratio of mean pressure over the pulse duration to peak pressure of the shock loading, for a sharper pulse shape usually causes damage to the structure easier than a flat pulse [4–7]. Thus, the former approach is not applicable in shock loading simulation, especially when the effect of pulse shape is remarkable. In fact, upon comparing the applicability of the two approaches on metallic sandwich plates, it was demonstrated that, beyond the impulsive regime, treating the pressure time history as a momentum would significantly overestimate core crushing and energy dissipation [2,3].

The technique of using uniform metal foam projectile to simulate shock loading [8–12] belongs to the former approach, namely, using impulse I to define the level of shock loading. However, the approach is insufficient to precisely simulate pressure time history (especially pulse shapes) in many practical cases and hence not applicable beyond the impulsive regime. The reason is that the pulse shapes generated by metal foam projectiles exhibit little difference. Specifically, when a uniform metal foam projectile with length L and density ρ_f is fired from a gas gun at velocity V_0, it produces a rectangular-liked time-dependent pressure pulse on a rigid stationary target [8]. Mathematically, this pressure pulse can be characterized by:

$$P_{peak} = \sigma_c + \frac{\rho_f V_0^2}{\varepsilon_D} \tag{1}$$

$$\tau = \frac{L\varepsilon_D}{V_0} \tag{2}$$

where σ_c and ε_D are the plateau stress and nominal densification strain of the metal foam. The pressure pulse remains rectangular in shape no matter how the design parameters (L, ρ_f, V_0) of the foam projectile are varied. Since the approach is such an economical and simple approach that it would thus be inspiring if alternative approaches could be developed to include the pulse shape design in shock loading simulations. Introducing density gradient into metal foam projectile may alter the simulated shock loading shape, thus providing a chance to generate shock loading with specific pulse shape and extend the foam projectile-based shock loading simulation approach to wider applications. However, it is not clear whether such idea is feasible, because no associated works can be used to support the idea directly.

Over the past few years, density graded metal foams have already been manufactured, which makes it possible to employ density-graded metal foam projectiles in simulating shock loadings. The electrochemical method was first used to prepare density-graded foams [13]. After that, Y. Matsumoto developed the chemical dissolution method to produce the open-cell reticulated aluminum foams with graded densities [14]. Yoshihiko utilized the friction stir technique to bond the aluminum plates with different TiH2 contents and foamed the obtained precursor to produce density-graded foams [15]. By this method, stepwise density gradient is achieved owing to the discrete foaming agent contents in the different layers of foamable precursor. Unlike the above methods, Orbulov use pressure infiltration technique to produce hybrid metal matrix syntactic foams [16–18]. Since the infilled hollow spheres can be easily controlled, it is quite easily to produce graded metal foams.

Under high loading rates, density graded metal foams have been proved to outperform their uniform counterparts in many applications [19–30]. For example, as sacrificial claddings, density gradient can improve the performance of energy absorption, and reduce the impulse or maximum stress transferred to the protected structures under impact, or blast [19–25]. Similarly, when density-graded metal foams are used as sandwich cores. It was found that a well-designed density gradient sequence can enhance the blast resistance of foam-cored sandwich constructions [26–30]. Liu [26] indicates that the density gradient sequence with larger density of foam layer at the blast side achieved the best performance in terms of the global deformation. Similar conclusion is obtained for the graded honeycomb-cored sandwich panels by Li [29,30] through combined experimental and numerical study. In [35], it was also indicated that the blast resistance of graded sandwich panels were also affected by the deformation modes, which should be paid much attention.

The underlying mechanism that density graded metal foams outperform their uniform counterparts may be due to that density gradient may influence shock wave propagation in metal foams. In recent years, several theoretical approaches based on the propagation of one-dimensional (1D) shock wave have been proposed to illustrate dynamic compaction wave propagation in density-graded metal foams. For instance, by assuming that the local stress-strain characteristics the foam can be described with the idealized rigid-perfectly plastic-locking (RPPL) model [31–33], the effect of graded plateau stress on both the quasi-static and dynamic responses of density-graded foam rods under impact loading was quantified [34,35]. The same method was adopted to study the propagation of compaction wave in density-graded cellular materials subjected to blast loading [36]. Also built upon the RPPL idealization, Liu [37] proposed another model for dynamic compaction of density-graded cellular materials and defined a predefined locking density from which the mass continuity and momentum conversation conditions can be applied. Instead of the RPPL model, the rigid-plastic-hardening (R-PH) idealization [38,39] was used to characterize the stress-strain relation of density-graded foams, with the effect of local strain hardening taken into account [40]. Besides, Karagiozova and Alves [41] developed an analytical approach to predict the dynamic response of density-graded foams by assuming the material stress-strain curve at any cross-section can be treated as an equivalent local characteristic Hugoniot representation. According to this representation, the stress-strain curve of the graded foam exhibits local strain hardening, in which the strain fields are functions of both the velocity variation and density distribution.

Until now, most studies focused on applications of density graded metal foams in cladding structures and sandwich cores while no work has reported their applications in shock loading simulation, especially in pulse shape design. From the viewpoint of compaction wave propagation in density graded foams, density gradient has the potential to alert the simulated shock loading shape, thus expanding the foam projectile-based shock loading simulation technique to wider applications. Motivated by this, the present work is carried out to explore the potential of using density-graded metal foam projectile in pulse shape design.

In the first, effect of density gradient on the pulse shape of pressure time histories generated by density-graded foam projectiles is

experimentally explored. Subsequently, the cell-based finite element (FE) models for density-graded metal foams are constructed. The impact of graded foam projectiles on a fixed rigid wall is then conducted to explore the potential and underlying mechanisms of density-graded metal foam projectiles in generating pressure pulses with various shapes. Based upon the FE simulations, the Taylor impact model for a density-graded bar is developed to predict the contact pressure between the projectile and rigid wall. Finally, a design approach based on the developed Taylor impact model is proposed to determine the properties of density-graded metal foam projectiles that can generate specific pressure pulses.

2. Experimental investigation

2.1. Density-graded metal foam projectiles

Density-graded cylindrical aluminum foam projectiles of length 50 mm and diameter 28.5 mm were electro-discharge machined from aluminum foam blocks. The density-graded aluminum foam block was manufactured by the coupling of melt foaming process and the solidification process [42]. In such method, industrial pure aluminum was melted in a steel mold and preserved at 680 °C, then 1.5 wt% Calcium granules were added in the melt with 10 min of stirring. The 300 °C pre-treated TiH_2 powders with different contents were dispersed into the aluminum melt. Then the cooling procedure was implemented before the foam melt completely grew. The density gradients are determined by controlling the TiH_2 contents and timing of the cooling process.

In the present study, foam projectiles of two density gradients and one uniform density gradient are prepared, as is shown in Fig. 1a. For each density gradient, nine specimens are prepared, of which three are used to measure the density gradient, and the rest are used in the quasi-static compression tests and direct impact tests, respectively. The average cell size for S3 is 3.2 mm; while the cell size varies from 1.5 mm to 2.4 mm for S1, and from 1.9 mm to 3.6 mm for S2. By cutting the specimens into five slices, the density of the slices at different location away from the bottom of the specimens are measured, the corresponding slope of density gradient (k) can be obtained, as is shown in Fig. 1b.

The quasi-static compressive responses of the specimens are presented in Fig. 1c, at a nominal strain rate of 0.0067 s^{-1}. It is shown that the density gradient leads to strain hardening of the stress-strain curves. Besides, larger density gradient results in more remarkable strain hardening. Unlike uniform foams that initial collapse occurs at both ends of the specimen and then distributes randomly, the compaction band of density graded foams initiated from the end with smaller density and then propagate towards the other end, as is seen in Fig. 1d. The same phenomenon is observed in [43,44], where the graded properties is achieved by varying cross-section.

2.2. Direct impact test

As is sketched in Fig. 2, the direct impact experiments, in which foam projectiles were fired at a strain gauged Split Hopkinson bar, were performed, with the pressure time histories measured at the impact end of the foam projectiles. The bar was made of aluminum with a density of 2700 kg/m^3. The foam projectiles were accelerated using a gas gun barrel of diameter 28.5 mm. After the foam projectiles impacted on the end of the bar, the contact pressure histories on the impacted end of the bar were measured via strain gauges placed approximately 285 mm from the impact end of the bar. And the firing velocity is measured by the laser velometer. Compared with the foam projectile, the bar is so long that the impact section of the bar can be treated as a rigid wall.

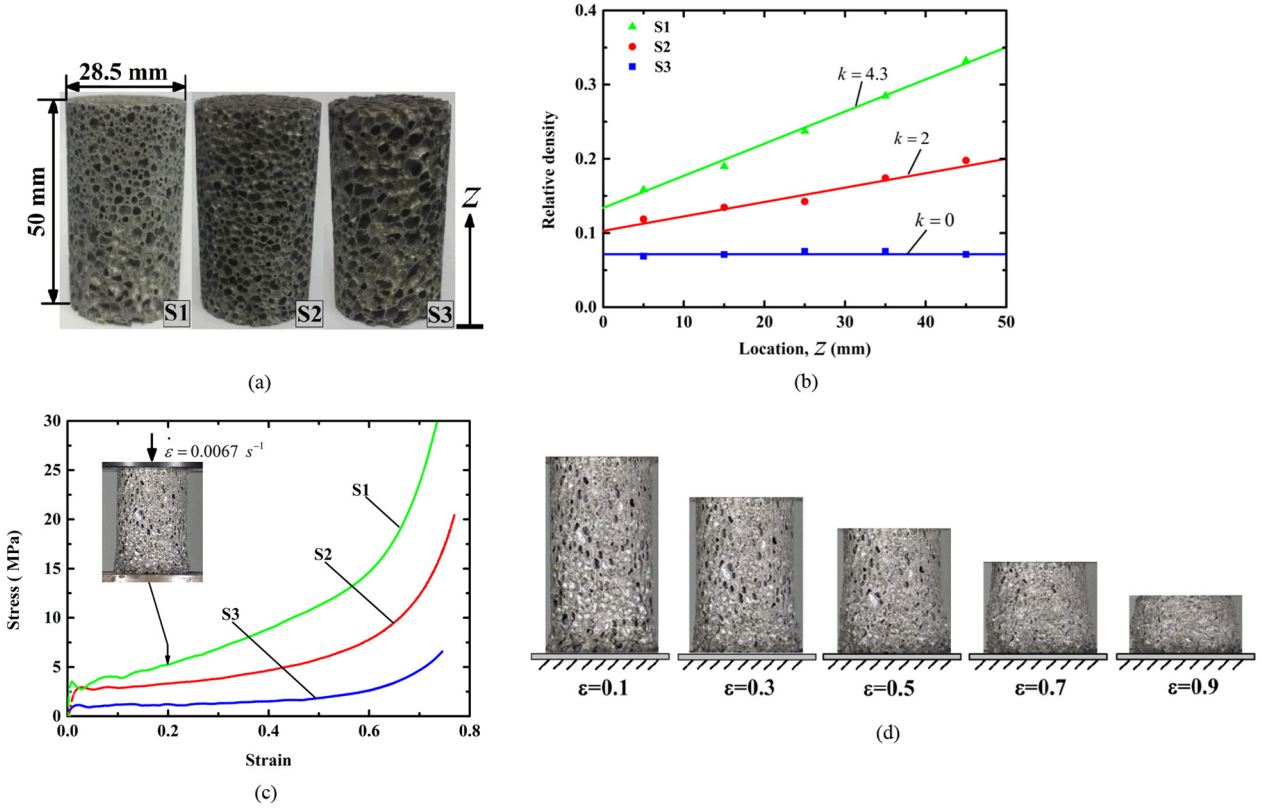

Fig. 1. (a) Morphology of density-graded aluminum foam testing specimens (specimen S1–S3). (b) Corresponding density gradients of specimens S1–S3. (c) Quasi-static compressive stress-strain curves of specimens S1–S3, each curve is an averaging of three specimens of same density gradient). (d) Quasi-static deformation process of density-graded metal foam specimen S1.

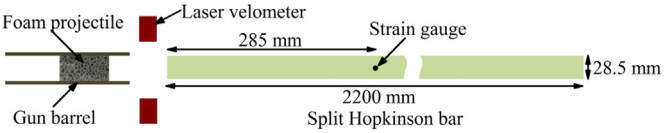

Fig. 2. Sketch of the direct impact Hopkinson bar setup.

2.3. Measurements

The measured pressure time histories of foam projectiles (S1–S3) are plotted in Fig. 3. In order to compare the pulse shape of the pressure time histories, the firing velocities of the projectiles are nearly the same, within 10% discrepancy. The firing velocity is controlled via the pressure of the gas in the chamber. It can be found from Fig. 3 that density gradient has significant influence on the pulse shape. Polynomial fitting curves of the pressure time histories show that the pulse shapes vary from rectangular-liked shape to triangular-liked shape and exponential-decayed-liked shape in sequence with the density gradient increases. It is also shown that the foam projectiles are not fully compacted under the prescribed firing velocities, which indicates that the foam projectiles are long enough to absorb their impact energy. Consequently, density-graded foam projectiles have the potential in generating shock loadings with various pulse shapes.

3. Cell-based finite element modeling

In the aforementioned section, a preliminary experimental study is carried out to explore the potential of density-graded foam projectiles in generating shock loadings with various pulse shapes. Since the firing velocities and mass of the foam projectiles in the experiments are different, the underlying mechanism that determines the pulse shape is not illustrated. In this section, the physical mechanism is investigated by cell-based finite element models.

3.1. Graded Voronoi foam

The 3D (three-dimensional) Voronoi technique is employed to generate closed-celled foam models with unique cell-wall thickness but graded cell sizes [45,46]. To this end, a total of N nuclei are placed in a 3D block, with the distance between any two nuclei larger than a minimum allowable distance, $r(z)$, which is a function of the Lagrange location z along the length of the Voronoi model. Accordingly, the block can be divided into N closed cells, and the boundaries of all the cells constitute the so-called δ-diagram, namely the Voronoi diagram with an irregularity degree of $\delta = r(z)/r_0$. Here, r_0 is the distance between two adjacent nuclei in a regular tetrakaidecahedral foam model with N cells in volume V, given by:

$$r_0 = \frac{\sqrt{6}}{2}\left(\frac{V}{\sqrt{2}N}\right)^{\frac{1}{3}} \tag{3}$$

Graded Voronoi structure is constructed by changing the distribution of cell size along the Lagrange location. With all the cell walls assumed to have a uniform thickness of h, the density of the j-th layer (within a minimum length of L/m, L being the length of the Voronoi structure and m the total number of foam layers in the structure) of the graded Voronoi structure is calculated by:

$$\rho_f(j) = \frac{\sum_{i=1}^{n} A_i^j \cdot h}{V/m} \cdot \rho_s \tag{4}$$

where n and A_i^j are the number of cell walls and area of the i-th cell wall in the j-th foam layer, respectively. And ρ_s denotes the density of parent material of foam.

3.2. Finite element modeling

Based on the Voronoi technique detailed above, a graded foam projectile specimen is constructed with a volume of $50 \times 28.5 \times 28.5$ mm^3, as shown in Fig. 4. The density $\rho_f(z)$ of the foam projectile is a function of the Lagrange location z from one end to another, as:

$$\rho_f(z) = (kz + b)\rho_s \tag{5}$$

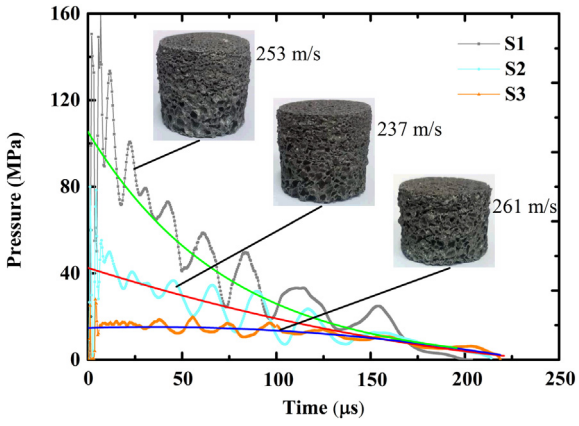

Fig. 3. The measured pressure time histories of the foam projectiles S1–S3, each curve is a single measurement for each firing velocity.

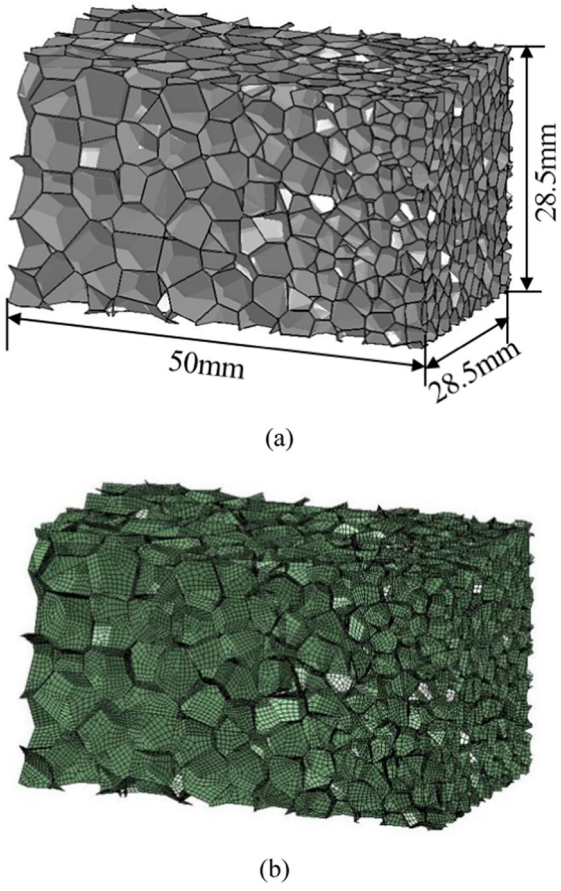

Fig. 4. (a) A 3D density-graded Voronoi foam structure in a volume of $50 \times 28.5 \times 28.5$ mm^3, (b) the corresponding cell-based finite element model.

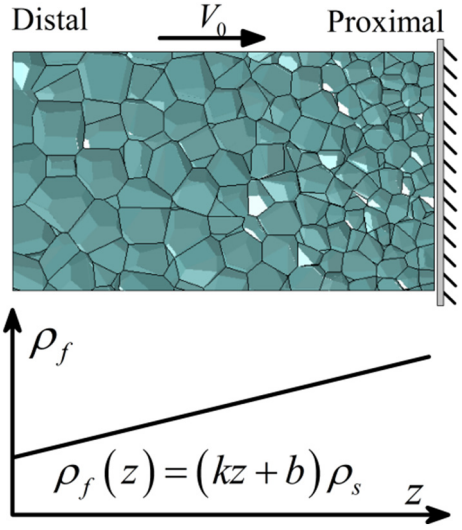

Fig. 5. Schematic of direct impact of density-graded foam projectile to fixed rigid wall.

where $k = 3$ and $b = 0.035$, with a unit of m^{-1}, k represents the slope of the density gradient. The irregularity δ of the Voronoi structure is set at 0.7. With reference to Fig. 5, let $z = 0$ correspond to the distal end of the projectile. Along the Lagrange location, the graded relative density increases linearly from 0.05 to 0.15. It is noticed that the cell size gradient is actually scattered in the m layers. The gradient may be treated as continuous when m is sufficiently large. In the current study, $m = 10$ is selected.

Full 3D finite element (FE) simulations are carried out with the commercialized software LS-DYNA. The graded Voronoi foam model is meshed by Shell 163 element with 5 integration points through the thickness. After numerous trials, the size of the element is eventually set to 0.2 mm to ensure mesh convergence. The parent material of cell walls is represented by a bilinear strain-hardening model as:

$$\sigma = \begin{cases} E_s\varepsilon, \varepsilon \le \dfrac{\sigma_{ys}}{E_s} \\ \sigma_{ys} + E_t\left(\varepsilon - \dfrac{\sigma_{ys}}{E_s}\right), \varepsilon > \dfrac{\sigma_{ys}}{E_s} \end{cases} \tag{6}$$

where σ_{ys} denotes the static yielding stress, and E_s and E_t are the Young's modulus and tangent modulus, respectively. The cell wall material used in the present study is aluminum, with mechanical properties listed in Table 1. For simplicity, strain-rate sensitivity of the material is not considered.

As shown in Fig. 5, to obtain the pressure-time history, full 3D impact simulation is considered in which the graded foam projectile impinges normally with an initial velocity V_0 on a stationary rigid wall. It should be noticed that the actual pressure imparted on the structure is somehow coupled with the deformation and movement of the target structure [8]. In the present study, we restrict our attention to the extreme case that the target is rigid and stationary, so as to purely explore the potential and underlying mechanisms of density gradient in the design of pulse shape. The present study considers a foam projectile whose density gradient is characterized by Eq. (5), with special focus placed upon the positive gradient ($k \ge 0$). During the dynamic simulations with LS-DYNA, contacts between the foam projectile and the target as well as those among the cell walls are considered with a fixed friction coefficient of 0.1 [45].

Table 1
Material properties of aluminum used in the present study.

E_s (GPa)	E_t (MPa)	σ_{ys} (MPa)	ρ_s (kg/m^3)	ν
69	58	100	2700	0.3

3.3. Validation of FE model

To validate the cell-based FE model, numerical results from direct impact simulations are compared with experimental results obtained for density-graded foam projectiles of $k = 0$ and $k = 2$. To maintain the same conditions as in experiment, cell-based foam models with density gradient $k = 0$ and $k = 2$ is constructed, respectively, and the fired velocity is 261 m/s and 237 m/s, correspondingly. As shown in Fig. 6, the pulse shape of the pressure-time history calculated from the present FE model is quite close to that of the experimental data, and the difference for the total momentum (i.e., the area below the pressure-time history) between FE calculations and experiments is less than 10%. It should be noticed that the foam projectile is cylinder in experiment but block in FE simulation, as shown in Fig. 5. However, the simulated pressure-time curve is less affected by the morphology of the foam projectile since there exists at least seven cells in any dimensional direction. Besides, the pressure-time curve is dominated by inertia stress enhancement which is affected by the density rather than the morphology. Therefore, the cell-based FE model is effective in representing the real closed-cell metallic foams.

In the section to follow, the significant effect of density gradient on the shape of the impact pulse generated by a foam projectile is investigated using the developed FE model.

3.4. Effect of foam density gradient on pressure-time history

With an initial velocity of 380 m/s, the numerically simulated evolution of the pressure exerted by foam projectile on rigid wall is plotted in Fig. 7 for selected density gradients of $k = 0$, $k = 1$ and $k = 3$. Unless otherwise stated, the average relative density and length of the foam projectiles is 0.11 and 50 mm, respectively. The results of Fig. 7 reveal that the pressure-time history generated by a density-graded foam projectile is no longer rectangular-liked, in contrast to that generated by a uniform foam projectile ($k = 0$). In fact, the graded foam projectile with a larger k usually generates a sharper pressure pulse with a higher peak pressure. Interestingly, however, while the density gradient affects significantly the profile of pressure pulse, it only has limited effect on the duration of the pulse, as shown in Fig. 7.

The above observations further demonstrate the great potential of employing the density gradient of metallic foam projectiles to design impact pulses with varying shapes, e.g., from rectangular-like shape to triangular and other shapes. The physical mechanisms underlying

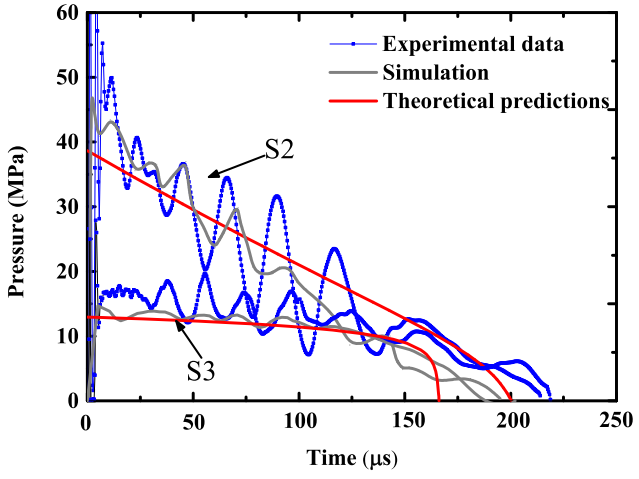

Fig. 6. Pressure-time histories obtained from predictions, cell-based FE simulation and experimental data (specimen S2 and S3).

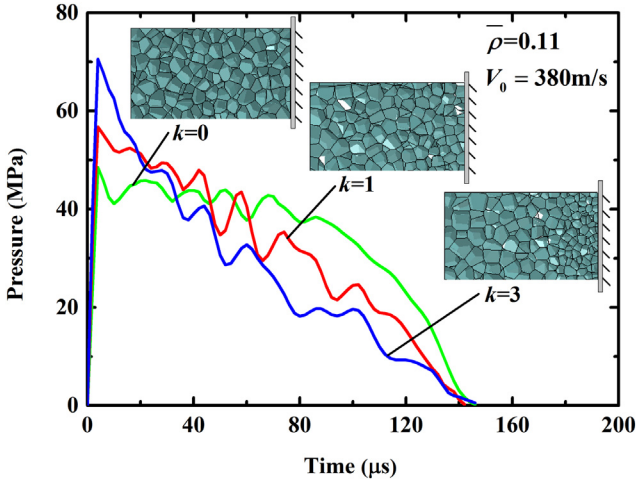

Fig. 7. Simulated pressure-time histories of metal foam projectiles with selected density gradients.

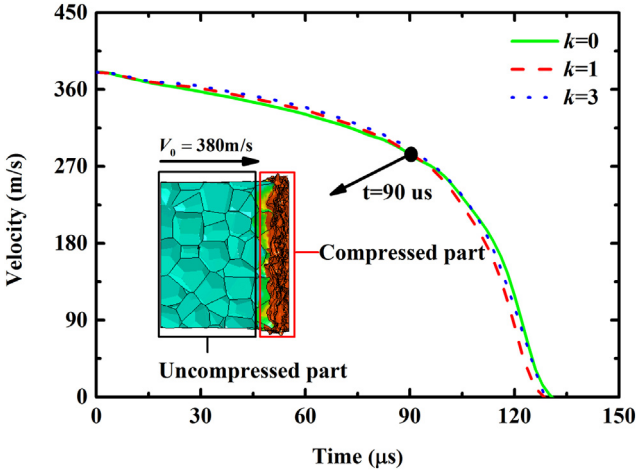

Fig. 9. Velocity-time history of the uncompressed part of density-graded foam projectile for $k = 0$, $k = 1$ and $k = 3$.

such influence of foam density gradient on pulse shape are explored next.

3.5. Physical mechanisms underlying the influence of density gradient

Fig. 8 presents the Lagrange locations of compaction band front (shock front) in density-graded metallic foam projectiles for $k = 0$, $k = 1$and $k = 3$; corresponding deformation pattern for the case of $k = 3$ is also presented. It is observed that the deformation pattern is 'shock-wave' where the band front propagates from the proximal end to the distal end. However, density gradient has little effect on the propagation of the band front, as shown in Fig. 8. Besides, the speeds of band front for both uniform and graded foam projectiles remain nearly constant before 100 us. After 120 us, the foam projectiles can no longer be compacted and the band fronts stop propagating. During the whole compaction process, the propagation of band front shows no difference for foam projectiles with either graded or uniform densities.

In addition to the speed of band front, density gradient also has little effect on the velocity (V) of the uncompressed part of the foam projectile, as shown in Fig. 9, in which the velocity-time histories of the uncompressed parts are plotted for $k = 0$, $k = 1$ and $k = 3$. The results of Fig. 9 reveal that the velocity of the uncompressed part decreases gradually during the impacting process.

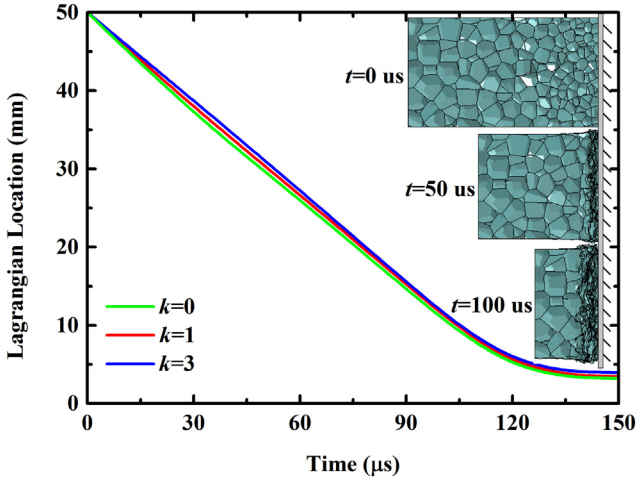

Fig. 8. Propagation of compaction band front in density-graded foam projectile for $k = 0$, $k = 1$ and $k = 3$. Corresponding deformation pattern is only displayed for $k = 3$.

The mechanisms underlying the pressure-time history of a foam projectile impacting a stationary rigid wall may be exploited by examining separately the quasi-static and dynamic compaction processes of the projectile. Based on full 3D FE simulations, the crushing stress of uniform Voronoi foam model subjected to quasi-static compression is

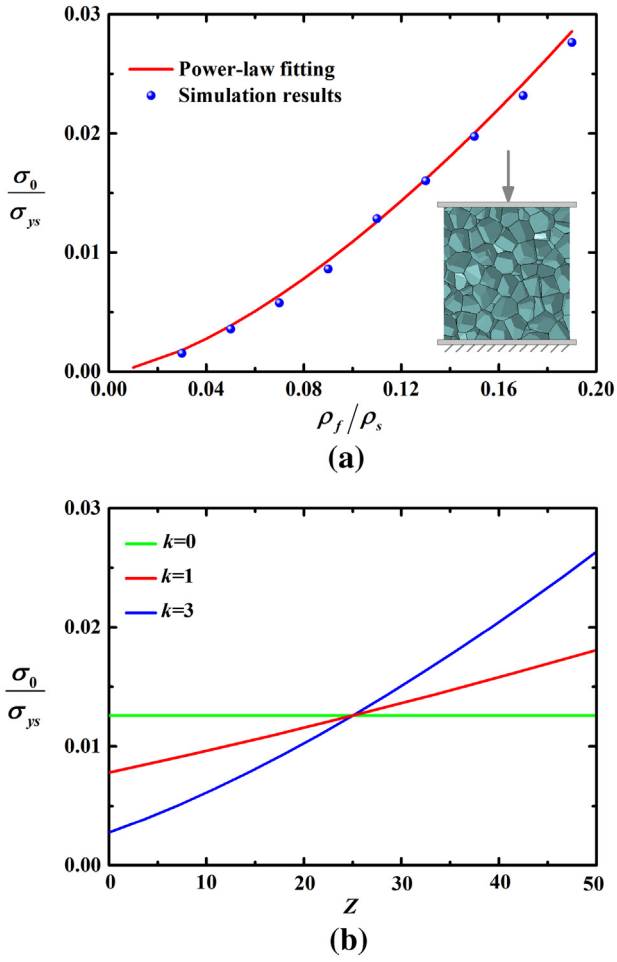

Fig. 10. (a) Normalized quasi-static crushing stresses of uniform foam plotted as a function of relative density: comparison between FE simulation and empirical power-law fitting; (b) Normalized quasi-static local crushing stress plotted as a function of Lagrange location of density-graded foam projectile.

plotted as a function of relative density (the varying density is controlled by cell size) in Fig. 10(a). For the purpose of comparison, the empirical crushing stress of closed-cell metallic foam obtained by fitting experimental data of quasi-static compression is given as [40]:

$$\sigma_0 = \alpha\left(\frac{\rho_f}{\rho_s}\right)^{\beta}\cdot\sigma_{ys} \tag{7}$$

which exhibits the format of power-law; α and β are the fitting constants. The results of Fig. 10(a) reveal that the empirical crushing stress of Eq. (7) agree well with the FE simulation results if $\alpha = 0.35$ and $\beta = 1.5$.

For density-graded foam projectiles, upon substituting ρ_f of Eq. (5) into Eq. (7), the local crushing stress along the Lagrange location z may be obtained as:

$$\sigma_0(z) = 0.35\left(\frac{kz+b}{\rho_s}\right)^{1.5}\cdot\sigma_{ys} \tag{8}$$

Based on Eq. (8), Fig. 10(b) presents the normalized local crushing stress along the Lagrange location of density-graded foam projectile for $k = 0$, $k = 1$ and $k = 3$. It can be concluded that the density gradient influences the shape of pressure pulse by changing the quasi-static part (i.e., the quasi-static crushing stress) of the pressure-time history.

Consider next the process of dynamic compaction. For each foam projectile ($k = 0, 1, 3$) considered, Fig. 11 presents the local density within the shock front (defined as ρ_f/ε_l in this study, ε_l being the dynamic locking strain detailed in Appendix A) at each instant. When the shock front propagates from the proximal end to the distal end, the local density is also changing with time, as depicted in Fig. 11. In the case of uniform foam projectile, the gradually increasing local density with time implies that the dynamic locking strain within the band front is gradually decreasing. In comparison, for density-graded foam projectiles, the decreasing of local density is attributed to both the decreasing density gradient along the Lagrange location and the increasing locking strain within the band front. Therefore, local density within the shock front is another factor affecting significantly the pulse shape.

In passing, it is noticed that the rapid rise of the curves at about 120 us in Fig. 11 is caused by the fact that the foam projectiles cannot be fully densified at the distal end.

Fig. 12 presents the dynamic stress due to inertial enhancement as a function of time for each foam projectile ($k = 0, 1, 3$) considered. The dynamic stress is calculated by $\rho_f V^2/\varepsilon_l$ from the data point in Figs. 9 and 11. Comparison between Figs. 12 and 7 indicates that the dynamic stress dominates the pressure-time history. Therefore, compared with

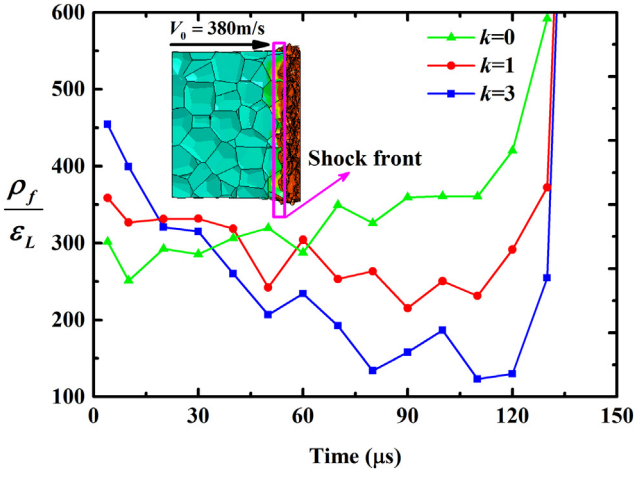

Fig. 11. Local density within shock front plotted as a function of time for density-graded foam projectiles with $k = 0$, $k = 1$ and $k = 3$.

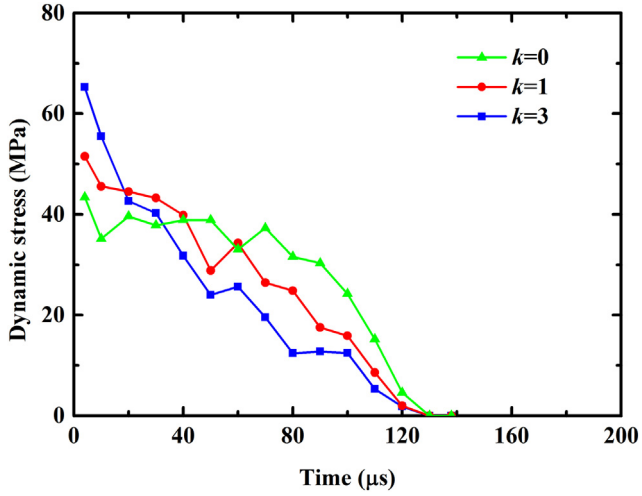

Fig. 12. The dynamic stress enhancement vs. time curves for density graded foams with density gradient $k = 0$, $k = 1$ and $k = 3$.

the varying density induced quasi-static crushing stress changes, the varying local density induced dynamic stress changes is the most important factor in altering pulse shapes.

4. Theoretical design of density-graded foam projectile

In the proceeding section, the potential and underlying mechanism of employing density-graded metal foam projectiles to generate shock loadings having different pulse shapes has been demonstrated using FE simulations. A theoretical approach based on the Taylor impact model is next developed to design graded metal foam projectiles and obtain pressure pulses having specific pulse shapes.

4.1. Taylor impact model with density-graded foam projectile

The direct impact of foam projectile on a stationary rigid wall is a typical problem of Taylor impact. There exist amount of theoretical works investigating the progressive compaction manner of cellular foam materials [31–33,38,39], of which the RPPL model [31–33] and the actual stress-strain curve based approach [38,39] are most applied. In the present study, the basic framework RPPL model is applied with additional assumptions. For a cell size induced density-graded metal foam projectile under high loading rates, it is assumed that the locking strain at any Lagrange location z can be approximated as $\varepsilon_l(z) = 1 - \lambda\rho_f(z)/\rho_s$. In other words, the densified density $\rho_d(z)$ of the density-graded metal foam at any Lagrange location is constant, i.e. $\rho_d(z) = \rho_s/\lambda$. The assumption is verified in Appendix A, in which the first order of locking strain $\varepsilon_l = 1 - \lambda\rho_f/\rho_s$ is in reasonable accordance with the numerical calculations based on 3D Voronoi foam models for $\lambda = 1.1$. Similar assumptions can be found in [35,37] where different coefficient λ is predefined.

Consider a cell size induced density-graded metal foam projectile, length L and cross-sectional area A, which impacts against the rigid wall with an initial velocity V_0, as depicted in Fig. 13. Upon impacting, the dynamic stress at the proximal end becomes sufficiently high to exceed the collapse stress of the foam, thus initiating a shock wave that propagates from the proximal end towards the distal end with the Eulerian speed of the shock front V_s. The mass conversation and the geometrical relationship are given, respectively, by

$$\int_0^z \rho_f(x)dx + \rho_d\int_0^t V_s dt = \int_0^L \rho_f(x)dx \tag{9}$$

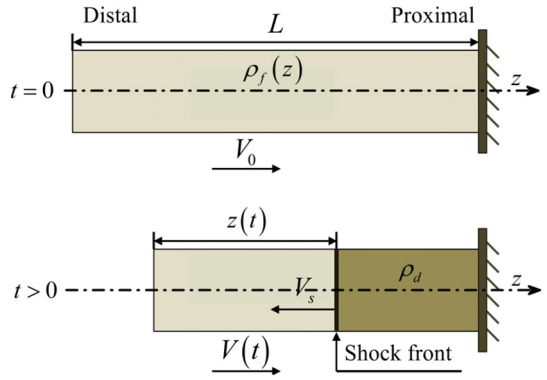

Fig. 13. A density-graded metallic foam projectile impacting against a stationary rigid wall.

$$z(t) = L - \int_0^t (V_s + V)dt \tag{10}$$

Differentiating Eqs. (9) and (10), we get

$$V(t) = \left(1 - \frac{\rho_f(z)}{\rho_d}\right)\frac{dz}{dt} \tag{11}$$

The conversation of the momentum of the portion ahead of shock front (the mass ahead of shock front is $\int_0^z \rho_f(x)dx$) gives:

$$-\sigma_0(z)dt = \int_0^z \rho_f(x)dx \cdot dV \tag{12}$$

Substituting $V(t)$ in Eq. (11) into Eq. (12) yields

$$\sigma_0(z) = \int_0^z \rho_f(x)dx \frac{d}{dt}\left\{\left[1 - \frac{\rho_f(z)}{\rho_d}\right]\frac{dz}{dt}\right\} \tag{13}$$

For a defined $\rho_f(z)$ in Eq. (5) and fitted $\sigma_0(z)$ in Eq. (8), the time-based parameters $z(t)$ and dz/dt can be obtained from Eq. (13) based on the four-order Runge-Kutta method in Matlab.

Given that the dynamic crushing stress behind shock front is σ_d, then the conversation of momentum of the total foam projectile gives:

$$-\sigma_d(z)dt = d\left[\int_0^z \rho_f(x)dx \cdot V\right] \tag{14}$$

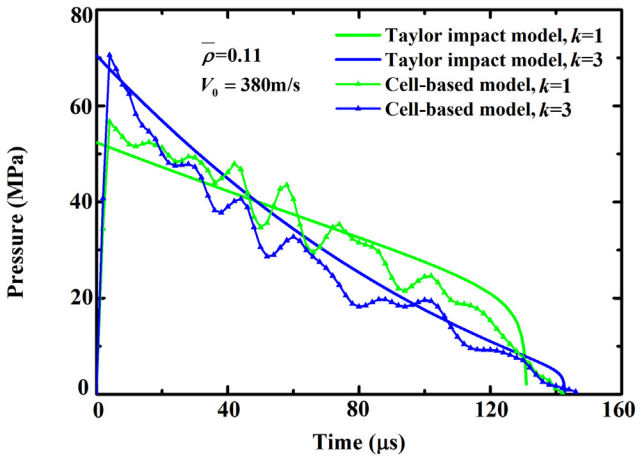

Fig. 14. Predicted pressure-time histories of density-graded metallic foam projectiles: comparison between 1D Taylor impact model and cell-based 3D FE model.

Substituting Eqs. (5) and (11) into Eq. (14), the pressure-time history of the density-graded foam projectile is given by:

$$P(t) = \sigma_0(z) + \rho_s(kz+b)[1-\lambda(kz+b)]\left(\frac{dz}{dt}\right)^2 \tag{15}$$

With the obtained time-based parameters $z(t)$ and dz/dt, the pressure-time history can be plotted according to Eq. (15).

In Fig. 6, theoretical model predictions by Eq. (15) are compared with experimental data as well as FE simulation results for metallic foam projectile with density gradient $k = 0$ and $k = 2$. Good agreement is achieved. For density-graded foam projectiles with gradients $k = 1$ and $k = 3$, in the absence of experimental data, Fig. 14 compares the pressure-time histories predicted by Eq. (15) and the FE simulations. Again, good agreement is achieved, thus demonstrating the effectiveness of the Taylor impact model for density-graded foam projectiles. In line with the FE simulations, the theoretical predictions of Eq. (15) also show that, as the density gradient is increased, the shape of the pressure pulse becomes sharper while the peak pressure is elevated.

Further insight into Eq. (15) shows that the pulse shape of shock loading is dependent upon a few parameters: the quasi-static local crushing stress $\sigma_0(z)$, the local density within shock front $\rho_f(z)/\varepsilon_l(z)$, and the square of real-time velocity of the uncompressed part $V^2(t)$. In the preceding sections, it has already been demonstrated that density gradient has little influence on the real-time velocity of the uncompressed part. Therefore, the pulse shape of shock loading is directly determined by the local crushing stress and local density of the foam projectile.

4.2. Design approach

In this section, based on the 1D Taylor impact model for graded metallic foams, a theoretical approach is developed to design foam projectiles that can generate pressure pulses having specific pulse shapes. Generally, to describe a shock loading with specific pulse shapes, three parameters are needed: total impulse (I), peak pressure (P_{peak}) and shape ratio (P_{mean}/P_{peak}).

According to Eq. (15), during the impacting process, the peak pressure and the mean pressure are given, respectively, as:

$$P_{peak} = P(t=0) = \sigma_0(L) + \frac{(kL+b)\rho_s {V_0}^2}{1-\lambda(kL+b)} \tag{16}$$

$$P_m = \frac{1}{\tau}\int_0^\tau P(t)dt \tag{17}$$

where τ denotes the duration of the pressure-time history generated by the graded foam projectile. Because density gradient has little effect on the duration of impact pulse as previously discussed, the modified Eq. (2) is adopted to represent the duration of pressure generated by a density-graded foam projectile, as:

$$\tau = \frac{L\overline{\varepsilon_l}}{V_0} \tag{18}$$

where $\overline{\varepsilon_l}$ denotes the mean value of locking strain along the foam projectile, given by:

$$\overline{\varepsilon_l} = \frac{1}{z}\int_0^z \varepsilon_l(x)dx \tag{19}$$

To illustrate the applicability of the theoretical approach outlined above in practical design, consider an idealized triangular pressure-time history with peak pressure 50 MPa and decay time 60 us, as depicted in Fig. 15. It follows that the total impulse per unit area and the shape ratio are 1.5 KPa·s, and 0.5, respectively. Correspondingly,

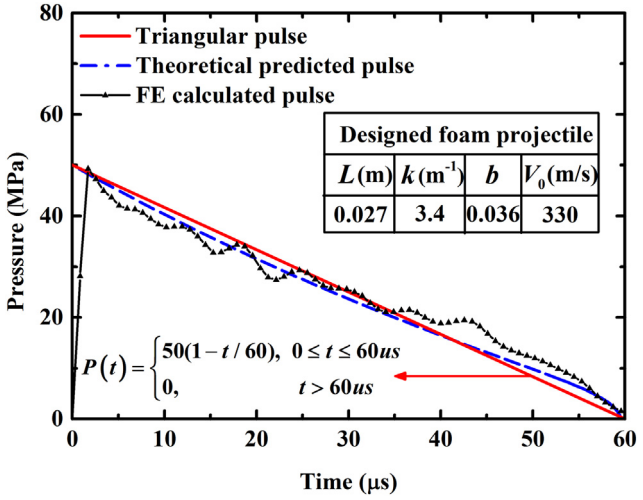

Fig. 15. Idealized triangular pressure pulse: theoretical model prediction and FE calculation based on purposely designed metallic foam projectile with density gradient ($k = 3.4$).

the geometric parameters (L, k, b) and initial velocity (V_0) of the graded foam projectile can be determined from the following equations:

$$\begin{cases} I = \overline{\rho_f} L \cdot V_0 = 1.5\text{KPa} \cdot \text{s} \\ \tau = \dfrac{L\overline{\varepsilon_l}}{V_0} = 60\mu\text{s} \\ P_m = \dfrac{1}{\tau}\displaystyle\int_0^{\tau} P(t)dt = 25\text{MPa} \\ P_{peak} = \sigma_0(L) + \dfrac{\rho_f(L){V_0}^2}{\varepsilon_l(L)} = 50\text{MPa} \\ \overline{\rho_f} = kL/2 + b, \rho_f(L) = kL + b \end{cases} \tag{20}$$

The results for (L, k, b, V_0) thus determined are displayed in Fig. 15. Upon substituting these parameters into the Taylor impact model (i.e., Eq. (15)), the pressure pulse can be obtained, as shown in Fig. 15. Meanwhile, based on the determined values of (L, k, b, V_0), the pressure-time history is calculated using FE simulations, which is also presented in Fig. 15.

The theoretically predicted and numerically calculated curves compare quite well with the desirable triangular pressure-time history, as shown in Fig. 15. Most features of the generated pressure pulse coincide with those of the prescribed curve, except for the decay rate. This deficiency can be improved by introducing nonlinear density gradient (e.g., quadratic and square root gradients) into the foam projectile, which is nonetheless beyond the scope of the current study.

5. Conclusions

Closed-cell metallic foam projectiles with graded relative densities are proposed to simulate shock loadings having varying pressure pulse shapes. The potential of density gradient in the design of pulse shape is exploited experimentally and numerically. Three-dimensional Voronoi foam models with varying gradient profiles along the length direction are constructed for FE simulations, which are validated against the experimental data. Subsequently, underlying physical mechanisms underlying the influence of density gradient on pulse shape are investigated using the validated simulation model. Based on the Taylor impact model, a theoretical approach is developed to design graded foam projectiles that generate pressure pulses with specific pulse shapes. The theoretical model predictions match well with full 3D numerical simulation results. The main conclusions drawn from the present study are:

- Manipulating with the density gradient of metallic foam projectiles is effective in pulse shape design. When the density gradient is increased, the shape of the pressure pulse becomes sharper and the peak pressure becomes higher, whereas the duration time remains unchanged.
- By introducing density gradient into metal foam projectiles, the shock loading simulation method introduced by Radford et al. [8] can be expanded from impulsive tests regime to dynamic tests regime.
- When the graded foam projectile impinges on a stationary rigid wall, the presence of density gradient induces changes not only in local crushing stress but also in dynamic stress enhancement due to inertial effect, of which the dynamic stress is the most important in determining the shape of pressure pulse generated during the impacting process.
- In practice, the theoretical approach developed in the current study can be employed to design the geometry and firing velocity of density-graded metallic foam projectile needed to generate a pressure pulse with prescribed shape.

CRediT authorship contribution statement

Lang Li: Conceptualization, Data curation, Formal analysis, Investigation, Writing - original draft, Writing-review & editing. **Bin Han:** Conceptualization, Writing-review & editing, Project administration. **Si-Yuan He:** Methodology, Resources. **Zhen-Yu Zhao:** Methodology, Software, Validation. **Rui Zhang:** Visualization, Data curation.
Qian-Cheng Zhang: Resources, Writing-review & editing, Project administration. **Tian Jian Lu:** Conceptualization, Supervision, Funding acquisition, Writing-review & editing.

CRediT authorship contribution statement

Lang Li: Conceptualization, Data curation, Formal analysis, Investigation, Writing - original draft, Writing-review & editing. **Bin Han:** Conceptualization, Writing-review & editing, Project administration. **Si-Yuan He:** Methodology, Resources. **Zhen-Yu Zhao:** Methodology, Software, Validation. **Rui Zhang:** Visualization, Data curation.
Qian-Cheng Zhang: Resources, Writing-review & editing, Project administration. **Tian Jian Lu:** Conceptualization, Supervision, Funding acquisition, Writing-review & editing.

Acknowledgments

This work was supported by the National Natural Science Foundation of China (11802221, 11472208, 11472209 and 11572087), the National Key R&D Program of China (2018YFB1106400), China Postdoctoral Science Foundation (2016M600782), Postdoctoral Scientific Research Project of Shaanxi Province (2016BSHYDZZ18), Zhejiang Provincial Natural Science Foundation of China (LGG18A020001), Natural Science Basic Research Plan in Shaanxi Province of China (2018JQ1078).

Appendix A. Determination of dynamic locking strain

Dynamic locking strain during the impacting process is investigated based on 3D Voronoi foam models, and the varying relative density is controlled by cell sizes. Based on simulation results, an empirical equation for the dynamic locking strain is given.

A series of 3D FE simulations for both quasi-static and dynamic compression (the prescribed constant velocity V_i varying from 100 m/s to 500 m/s) are carried out using Voronoi foam models for a large range of relative density (cell sizes). The crushing stress for quasi-static compression, σ_{cr}^{qs}, and that for dynamic compression, σ_{cr}^{d}, are obtained from the calculated compressive stress versus strain curves. These results are then used to calculate the locking strain based on 1D shock theory, as [47]:

$$\varepsilon_l = \frac{\rho_f {V_i}^2}{\sigma_{cr}^{d} - \sigma_{cr}^{qs}}. \tag{A1}$$

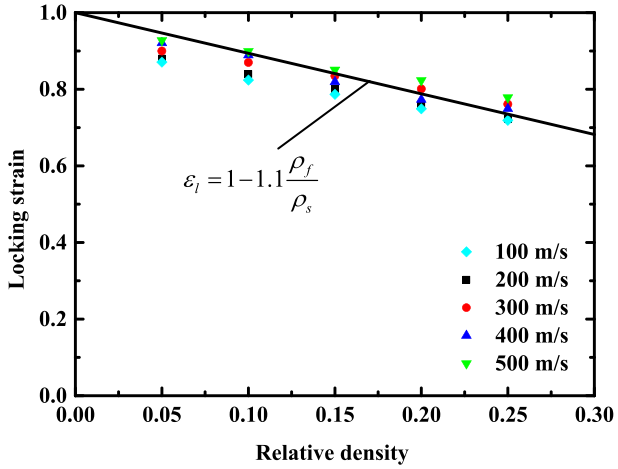

Fig. A1. Numerically calculated locking strain plotted as a function of foam relative density for selected impact velocities. Equation shown is obtained via curve fitting.

The locking strain calculated from Eq. (A1) is plotted in Fig. A1 as a function of relative density for closed-cell aluminum foams, with a range of impact velocities (from 100 m/s to 500 m/s) considered. It is seen that the locking strain is significantly dependent upon the foam relative density, decreasing linearly with increasing relative density, but is little affected by the impact velocity (at least in the velocity range considered here). Consequently, as a good approximation, the first order of theoretical prediction of the quasi-static densification strain ($\varepsilon_d = 1 - \lambda\rho_f/\rho_s$) may be used to imitate the dynamic locking strain. Thus the dynamic locking strain is given as:.

$$\varepsilon_l = 1 - \lambda\frac{\rho_f}{\rho_s} \tag{A2}$$

In view of the FE simulation results shown in Fig. A1, the best fit of Eq. (2).

gives $\lambda = 1.1$.

References

[1] G.R. Abrahamson, H.E. Lindberg, G.R. Abrahamson, Peak load-impulse characterization of critical pulse loads in structural dynamics, Nucl. Eng. Des. 37 (1976) 35–46.
[2] N. Jones, Structural Impact, Cambridge University Press, 1989.
[3] Z. Xue, J.W. Hutchinson, Preliminary assessment of sandwich plates subject to blast loads, Int. J. Mech. Sci. 45 (2003) 687–705.
[4] A. Vaziri, J.W. Hutchinson, Metal sandwich plates subject to intense air shocks, Int. J. Solids Struct. 44 (2007) 2021–2035.
[5] Q.M. Li, H. Meng, Pulse loading shape effects on pressure–impulse diagram of an elastic-plastic, single-degree-of-freedom structural model, Int. J. Mech. Sci. 44 (2002) 1985–1998.
[6] J.R. Florek, H. Benaroya, Pulse-pressure loading effects on aviation and general engineering structures-review, J. Sound Vib. 284 (2005) 421–453.
[7] G. Zhu, Y.G. Huang, T.X. Yu, Estimation of the plastic structural response under impact, Int. J. Impact Eng. 4 (2015) 271–282.
[8] D.D. Radford, V.S. Deshpande, N.A. Fleck, The use of metal foam projectiles to simulate shock loading on a structure, Int. J. Impact Eng. 31 (2005) 1152–1171.
[9] H.J. Rathbun, D.D. Radford, Z. Xue, M.Y. He, J. Yang, V. Deshpande, N.A. Fleck, J.W. Hutchinson, F.W. Zok, A.G. Evans, Performance of metallic honeycomb-core sandwich beams under shock loading, Int. J. Solids Struct. 43 (2006) 1746–1763.
[10] G.J. McShane, D.D. Radford, V.S. Deshpande, N.A. Fleck, The response of clamped sandwich plates with lattice cores subjected to shock loading, Eur. J. Mech. A. Solids 25 (2006) 215–229.
[11] D.D. Radford, N.A. Fleck, V.S. Deshpande, The response of clamped sandwich beams subjected to shock loading, Int. J. Impact Eng. 32 (2006) 968–987.
[12] M.A. Yahaya, D. Ruan, G. Lu, M.S. Dargusch, Response of aluminium honeycomb sandwich panels subjected to foam projectile impact-an experimental study, Int. J. Impact Eng. 75 (2015) 100–109.
[13] A. Neubrand, Electrochemical processing of porosity gradients for the production of functionally graded materials, J. Appl. Electrochem. 28 (1998) 1179–1188.
[14] Y. Matsumoto, A.H. Brothers, S.R. Stock, D.C. Dunand, Uniform and graded chemical milling of aluminum foams, Mater. Sci. Eng. A 447 (2007) 150–157.
[15] Y. Hangai, K. Takahashi, T. Utsunomiya, S. Utsunomiya, et al., Fabrication of functionally graded aluminum foam using aluminum alloy die castings by friction stir processing, Mater. Sci. Eng. A 534 (2012) 716–719.
[16] K. Májlinger, I.N. Orbulov, Characteristic compressive properties of hybrid metal matrix syntactic foams, Mater. Sci. Eng. A 606 (2014) 248–256.
[17] I.N. Orbulov, K. Májlinger, Characterisation of hybrid metal matrix syntactic foams, Mater. Sci. Forum 812 (2015) 219–222.
[18] A. Szlancsik, B. Katona, K. Bobor, K. Májlinger, I.N. Orbulov, Compressive behaviour of aluminium matrix syntactic foams reinforced by iron hollow spheres, Mater. Des. 83 (2015) 230–237.
[19] G.W. Ma, Z.Q. Ye, Energy absorption of double-layer foam cladding for blast alleviation, Int. J. Impact Eng. 34 (2007) 329–347.
[20] J.A. Main, G.A. Gazonas, Uniaxial crushing of sandwich plates under air blast: influence of mass distribution, Int. J. Solids Struct. 45 (2008) 2297–2321.
[21] L.L. Yan, Z.Y. Zhao, B. Han, T.J. Lu, B.H. Lu, Tube enhanced foam: a novel way for aluminum foam enhancement, Mater. Lett. 227 (2018) 70–73.
[22] D.D. Radford, G.J. McShane, V.S. Deshpande, N.A. Fleck, The response of clamped sandwich plates with metallic foam cores to simulated blast loading, Int. J. Solids Struct. 43 (2006) 2243–2259.
[23] W. Hou, F. Zhu, G. Lu, D.N. Fang, Ballistic impact experiments of metallic sandwich panels with aluminium foam core, Int. J. Impact Eng. 37 (2010) 1045–1055.
[24] M.S.H. Fatt, H. Surabhi, Blast resistance and energy absorption of foam-core cylindrical sandwich shells under external blast, Compos. Struct. 94 (2012) 3174–3185.
[25] L.L. Yan, B. Yu, B. Han, Q.C. Zhang, T.J. Lu, B.H. Lu, Effects of aluminum foam filling on low velocity impact response of sandwich panel with corrugated cores, J. Sandw. Struct. Mater. (2018)https://doi.org/10.1177/1099636218776585 (1099636218776585).
[26] X. Liu, X. Tian, T.J. Lu, D. Zhou, B. Liang, Blast resistance of sandwich-walled hollow cylinders with graded metallic foam cores, Compos. Struct. 94 (2012) 2485–2493.
[27] J.D. Li, G.W. Ma, H.Y. Zhou, X.L. Du, Energy absorption analysis of density graded aluminium foam, Int. J. Pro. Struct. 2 (2011) 333–349.
[28] J.J. Zhang, Z.H. Wang, L.M. Zhao, Dynamic response of functionally graded cellular materials based on the Voronoi model, Compos. Part B 85 (2016) 176–187.
[29] S. Li, X. Li, Z. Wang, et al., Sandwich panels with layered graded aluminum honeycomb cores under blast loading, Compos. Struct. 173 (2017) 242–254.
[30] S. Li, X. Li, Z. Wang, et al., Finite element analysis of sandwich panels with stepwise graded aluminum honeycomb cores under blast loading, Compos. Part A 80 (2016) 1–12.
[31] S.R. Reid, C. Peng, Dynamic uniaxial crushing of wood, Int. J. Impact Eng. 19 (1997) 531–570.
[32] P.J. Tan, S.R. Reid, J.J. Harrigan, Z. Zou, S. Li, Dynamic compressive strength properties of aluminium foams. Part i—experimental data and observations, J. Mech. Phys. Solids 53 (2005) 2174–2205.
[33] P.J. Tan, S.R. Reid, J.J. Harrigan, Z. Zou, S. Li, Dynamic compressive strength properties of aluminium foams. Part II – 'shock' theory and comparison with experimental data and numerical models, J. Mech. Phys. Solids 53 (2005) 2206–2230.
[34] C.J. Shen, T.X. Yu, G. Lu, Double shock mode in graded cellular rod under impact, Int. J. Solids Struct. 50 (2013) 217–233.
[35] C.J. Shen, G. Lu, T.X. Yu, Investigation into the behavior of a graded cellular rod under impact, Int. J. Impact Eng. 74 (2014) 92–106.
[36] M. Liang, Z. Li, F. Lu, X. Li, Theoretical and numerical investigation of blast responses of continuous-density-graded cellular materials, Compos. Struct. 164 (2017).
[37] J. Liu, B. Hou, F. Lu, H. Zhao, A theoretical study of shock front propagation in the density-graded cellular rods, Int. J. Impact Eng. 80 (2015) 133–142.
[38] Z. Zheng, J. Yu, C. Wang, S. Liao, Y. Liu, Dynamic crushing of cellular materials: a unified framework of plastic shock wave models, Int. J. Impact Eng. 42 (2012) 66–79.
[39] D. Karagiozova, G.S. Langdon, G.N. Nurick, Propagation of compaction waves in metal foams exhibiting strain hardening, Int. J. Solids Struct. 49 (2012) 2763–2777.
[40] J. Yang, S. Wang, Y. Ding, Z. Zheng, J. Yu, Crashworthiness of graded cellular materials: a design strategy based on a nonlinear plastic shock model, Mater. Sci. Eng. A (2016) 680.
[41] D. Karagiozova, M. Alves, Propagation of compaction waves in cellular materials with continuously varying density, Int. J. Solids Struct. 71 (2015) 323–337.
[42] S.Y. He, Y. Zhang, G. Dai, J.Q. Jiang, Preparation of density-graded aluminum foam, Mater. Sci. Eng. A 618 (2014) 496–499.
[43] C.J. Shen, G. Lu, T.X. Yu, D. Ruan, Dynamic response of a cellular block with varying cross-section, Int. J. Impact Eng. 79 (2015) 53–64.
[44] C.J. Shen, G. Lu, D. Ruan, T.X. Yu, Propagation of the compaction waves in a cellular block with varying cross-section, Int. J. Solids Struct. 88 (2016) 319–336.
[45] L. Li, P. Xue, G. Luo, A numerical study on deformation mode and strength enhancement of metal foam under dynamic loading, Mater. Des. 110 (2016) 72–79.
[46] B. Han, B. Yu, R.P. Yu, Q.C. Zhang, H.J. Gao, Q. Zhang, T.J. Lu, B.H. Lu, Creep of closed-cell aluminum foams: effects of imperfections and predictive modeling, Mater. Des. 156 (2018) 229–241.
[47] P.J. Tan, S.R. Reid, J.J. Harrigan, On the dynamic mechanical properties of open-cell metal foams–a re-assessment of the 'simple-shock theory', Int. J. Solids Struct. 49 (2012) 2744–2753.